The Astrophysical Journal, 756:159 (10pp), 2012 September 10 doi:10.1088/0004-637X/756/2/159

A BRIGHTEST CLUSTER GALAXY WITH AN EXTREMELY LARGE FLAT CORE

Marc Postman[1], Tod R. Lauer[2], Megan Donahue[3], Genevieve Graves[4], Dan Coe[1], John Moustakas[5,6], Anton Koekemoer[1], Larry Bradley[1], Holland C. Ford[7], Claudio Grillo[8], Adi Zitrin[9], Doron Lemze[7], Tom Broadhurst[10,11], Leonidas Moustakas[12], Begoña Ascaso[13], Elinor Medezinski[7], and Daniel Kelson[14]
[1] Space Telescope Science Institute, 3700 San Martin Drive, Baltimore, MD 21208, USA
[2] National Optical Astronomy Observatory, P.O. Box 26732, Tucson, AZ 85726, USA
[3] Department of Physics and Astronomy, Michigan State University, East Lansing, MI 48824, USA
[4] Department of Astronomy, 601 Campbell Hall, University of California, Berkeley, CA 94720, USA
[5] Center for Astrophysics and Space Sciences, University of California, La Jolla, CA 92093, USA
[6] Department of Physics and Astronomy, Siena College, 515 Loudon Road, Loudonville, NY 12211, USA
[7] Department of Physics & Astronomy, Johns Hopkins University, 3400 North Charles Street, Baltimore, MD 21218, USA
[8] Dark Cosmology Centre, Niels Bohr Institute, University of Copenhagen, Juliane Mariesvej 30, DK-2100 Copenhagen, Denmark
[9] University of Heidelberg, Albert-Ueberle-Str. 2, D-69120 Heidelberg, Germany
[10] Department of Theoretical Physics, University of the Basque Country UPV/EHU, Bizkaia, E-48940 Leioa, Spain
[11] IKERBASQUE, Basque Foundation for Science, Alameda Urquijo 36-5, E-48008 Bilbao, Spain
[12] Jet Propulsion Laboratory, California Institute of Technology, 4800 Oak Grove Drive, Pasadena, CA 91109, USA
[13] Instituto de Astrofísica de Andalucía (CSIC), C/Camino Bajo de Huétor 24, E-18008 Granada, Spain
[14] The Observatories of the Carnegie Institution of Washington, 813 Santa Barbara Street, Pasadena, CA 91101, USA
Received 2012 May 16; accepted 2012 July 24; published 2012 August 24

ABSTRACT

Hubble Space Telescope images of the galaxy cluster A2261, obtained as part of the Cluster Lensing And Supernova survey with Hubble, show that the brightest galaxy in the cluster, A2261-BCG, has the largest core yet detected in any galaxy. The cusp radius of A2261-BCG is 3.2 kpc, twice as big as the next largest core known, and ∼3× bigger than those typically seen in the most luminous brightest cluster galaxies. The morphology of the core in A2261-BCG is also unusual, having a completely flat interior surface brightness profile, rather than the typical shallow cusp rising into the center. This implies that the galaxy has a core with constant or even centrally decreasing stellar density. Interpretation of the core as an end product of the "scouring" action of a binary supermassive black hole implies a total black hole mass $\sim 10^{10}\ M_{\odot}$ from the extrapolation of most relationships between core structure and black hole mass. The core falls 1σ above the cusp radius versus galaxy luminosity relation. Its large size in real terms, and the extremely large black hole mass required to generate it, raises the possibility that the core has been enlarged by additional processes, such as the ejection of the black holes that originally generated the core. The flat central stellar density profile is consistent with this hypothesis. The core is also displaced by 0.7 kpc from the center of the surrounding envelope, consistent with a local dynamical perturbation of the core.

Key words: galaxies: nuclei – galaxies: photometry – galaxies: structure

Online-only material: color figures

1. A LARGE CORE AS A TEST OF CORE FORMATION

Brightest cluster galaxies (BCGs) and most luminous early-type galaxies brighter than $M_V \sim -21$ have "cores" in their central starlight distributions (Faber et al. 1997; Laine et al. 2002; Lauer et al. 2007a). Cores are marked by a distinct physical radius interior to which the projected starlight surface brightness increases only slowly as $r \rightarrow 0$, in marked contrast to the surrounding envelope, which has a much steeper profile (in logarithmic units). In qualitative terms, a core looks like a central "plateau" in the starlight distribution. In more quantitative terms, a core can be defined as the central region of a galaxy where the surface brightness takes the form of a shallow cusp, $I(r) \propto r^{-\gamma}$, with $\gamma < 0.3$ as $r \rightarrow 0$ (Lauer et al. 1995, 2005). Importantly, galaxies fainter than $M_V \sim -21$ generally do not have cores, having $\gamma > 0.5$ instead, as $r \rightarrow 0$. This distinction is of physical interest, as the presence or absence of a core correlates with the strength of the stellar rotation field, isophote shape, nuclear radio emission, and overall X-ray emission, in addition to the total galaxy luminosity (Faber et al. 1997; Lauer et al. 2007b).

The formation of cores has long been thought to be due to the action of black holes on the central structure of galaxies. Their form and size may reflect both the mass of the central black hole in the galaxies and the merger history that created the galaxies. Begelman et al. (1980) hypothesized that a binary black hole created in the merger of two galaxies would eject stars from the center of the newly created system as the binary slowly hardened. In simple terms, the black hole binary "scours" out the center of the galaxy, thus "flattening" the otherwise steeply rising central starlight distribution as $r \rightarrow 0$. Subsequent N-body simulations have demonstrated this phenomenon directly (Ebisuzaki et al. 1991; Makino 1997; Milosavljević & Merritt 2001).

Faber et al. (1997) showed that cores occur in the most luminous elliptical galaxies and are correlated with slow-rotation and "boxy" isophotes in these galaxies, concluding that core formation is a natural end-point of dissipationless mergers of two progenitor elliptical galaxies. The conclusion that nearly every elliptical galaxy has a black hole at its center (Magorrian et al. 1998), coupled with the conclusion that the most massive elliptical galaxies were formed by merging pre-existing gas-free galaxies, explains why cores are found in nearly all luminous ellipticals.

While "core scouring" is an attractive hypothesis for the formation of cores, there may be additional mechanisms for binary black holes to generate cores. Redmount & Rees (1989)

suggested that when the two black holes in the binary ultimately merge, asymmetric emission of gravitational radiation could eject the merged hole from the center of the galaxy, causing the center to "rebound" in response to the large reduction in central mass. Merritt et al. (2004), Boylan-Kolchin et al. (2004), and Gualandris & Merritt (2008) studied this problem in detail for realistic galaxy models, demonstrating that the ejection of the merged black hole indeed could cause the central distribution of starlight to re-adjust such that it would create a core in the projected stellar surface brightness profile. An interesting ancillary effect discussed in these works is the possibility that the ejected black hole would remain bound to the host galaxy on a radial orbit. In that case, it would repeatedly fall through the center of the galaxy, continuing to enlarge the core through dynamical friction.

Some observational support for the scouring origin of cores comes from the measurement of core "mass deficits" compared to the black hole masses in the same galaxies (Faber et al. 1997). The mass deficit, M_d, is the inferred mass of stars ejected from the center of the galaxy requited to create a core and is estimated by a reference to a postulated initial form of the galaxy fitted to the envelope, such as a Sérsic law (Graham 2004). Various studies estimating mass deficits (Faber et al. 1997; Milosavljević et al. 2002; Ravindranath et al. 2002; Graham 2004; Merritt 2006; Lauer et al. 2007a; Kormendy & Bender 2009) typically find $M_d \propto M_\bullet$, the black hole mass, with the constant of proportionality of order unity, but with large scatter about the mean relation.

The observational context for understanding the large core in the BCG in A2261 (hereafter referred to as A2261-BCG) is provided by the extensive work done with the *Hubble Space Telescope* (*HST*) on the structure of nearby galaxies. Lauer et al. (2007a) constructed a large sample of galaxies that had high-resolution surface photometry obtained with *HST;* significantly, it included the core parameters measured by Laine et al. (2002), who studied a large sample of BCGs. Very few galaxies have cores as large as 1 kpc; the largest core in the Lauer et al. (2007a) sample is that for NGC 6166 = A2199-BCG, which has a core size of ∼1.5 kpc. McNamara et al. (2009) drew attention to the large core that they discovered in BCG MS0735.6+7421; however, it is compatible with the largest BCG cores measured in the Laine et al. (2002) sample. The core in A2261-BCG, however, is over twice as large as that in NGC 6166. It provides an extreme test of the possible mechanisms hypothesized to generate cores.

2. OBSERVATIONS AND PROPERTIES OF A2261-BCG

The center of A2261 was observed for a total of 20 orbits as part of the Cluster Lensing And Supernova survey with Hubble (CLASH) multi-cycle treasury program between 2011 March 9 and 2011 May 21 in 16 broadband filters from 0.22 to 1.6 μm (Postman et al. 2012). For the calculation of physical quantities, we assume a cosmology with $\Omega_m = 0.3$, $\Omega_\Lambda = 0.7$, and $H_0 = 70$ km s^{-1} Mpc^{-1}. At the mean redshift of A2261, $z = 0.2248$ (Coe et al. 2012), 1″ subtends 3.61 kpc and the distance modulus is 40.241.

A2261 is included in the CLASH X-ray-selected subsample of 20 clusters. The CLASH X-ray-selected sample consists of clusters with X-ray temperatures greater than 5 keV and exhibits a high degree of dynamical relaxation as evidenced by *Chandra X-Ray Observatory* images that show well-defined central surface brightness peaks and nearly concentric isophotes. The intracluster medium (ICM) of A2261, in particular, is characterized by an X-ray temperature of $T_x = 7.6 \pm 0.30$ keV, a bolometric X-ray luminosity of $1.80 \pm 0.20 \times 10^{45}$ erg s^{-1}, and an [Fe/H] abundance ratio that is 0.31 ± 0.06 times the solar value (Anders & Grevesse 1989). The estimated mass within r_{2500} (radius where the density is 2500 times the critical density) is $M_{2500} = (2.9 \pm 0.5) \times 10^{14}\, M_\odot$ with a gas fraction of 0.115 ± 0.01.

Maughan et al. (2008) found A2261 to have a small level of substructure in its X-ray gas surface brightness distribution and Gilmour et al. (2009) classified the cluster as "disturbed." Coe et al. (2012) find that application of the caustic technique (e.g., Diaferio & Geller 1997; Diaferio et al. 2005) to spectroscopically measured galaxies in the vicinity of A2261 suggests that the dynamical center of the cluster is located ∼6′ (∼1.3 Mpc) south of the BCG. However, the BCG ($z = 0.2233$) in A2261 is at equatorial coordinates of 17:22:27.18 +32:07:57.1 (J2000), putting it within 1.″6 (5.8 kpc) of the centroid of the ICM X-ray emission. Its mean velocity offset relative to that of the cluster mean redshift is 367 km s^{-1}. The distribution of BCG velocity offsets for a sample of 42 Abell clusters has a mean value of 264 km s^{-1} (Postman & Lauer 1995). An expanded data set of 174 Abell clusters, each with at least 50 spectroscopically confirmed members, yields a mean value of the BCG velocity offset of 234 km s^{-1}, with 22% having offsets of at least 350 km s^{-1}. The A2261-BCG, thus, appears to be reasonably aligned with the center of the cluster's main gravitational potential well.

The unusual core of A2261-BCG was discovered during the initial inspection of the CLASH *HST* images of A2261. Visually, the core presents itself as a large, round, uniform disk of low surface brightness, as can be seen in Figure 1, which shows a color composite of the central 2′ × 2′ region of A2261 made from the CLASH images. In addition, four compact sources with colors similar to the BCG itself are superimposed on the outskirts of the core. The three brightest knots are marginally detected ($<3\sigma$) in the WFC3/UVIS F336W image, well detected ($>6\sigma$) at longer wavelengths, and not detected in either the F225W or F275W UVIS passbands.

2.1. Nuclear Activity

Understanding the central structure of A2261-BCG requires knowledge of whether or not the core hosts a central supermassive black hole. This problem will be considered at length later in the paper, but we note here that the center of the galaxy does harbor a radio source that is at least an order of magnitude more powerful than those associated with star-forming regions and is thus evidence in favor of an active galactic nucleus (AGN). The NRAO VLA Sky Survey (NVSS; Condon et al. 1998) finds a source at 1.4 GHz with an integrated flux of 5.3 ± 0.5 mJy that lies 6.″3 east of the BCG position. No other NVSS sources are found within 2.′45 of the BCG. Data from the Faint Images of the Radio Sky at Twenty Centimeters (FIRST) survey (White et al. 1997) reveals a 3.4 mJy source that is more coincident with the core, lying 1.″6 west of the BCG position. The FIRST detection limit at the source position is 0.99 mJy beam^{-1}. No other FIRST sources are found within 1.′92 of the BCG. Presumably the NVSS and FIRST detections closest to the BCG correspond to the same source. The two radio positions are 7.″5 apart, which is less than a 2σ difference and is consistent with the different astrometric uncertainties for the two surveys. Unfortunately, the Very Large Array (VLA) sky survey data currently do not have sufficient angular resolution to determine whether one of the knots, or the core itself, may host the AGN (VLA FIRST resolution is 5″, NVSS resolution is 45″).

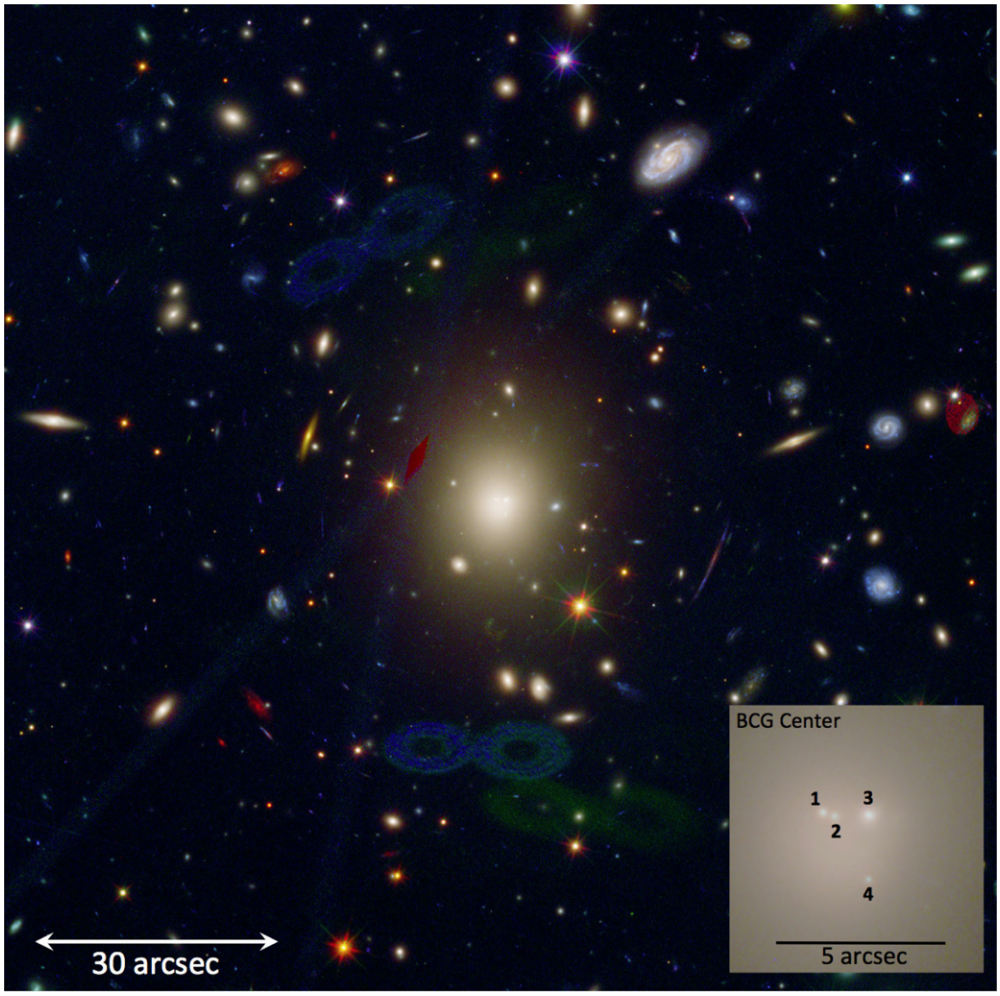

Figure 1. Color composite *HST* image, from CLASH ACS/WFC and WFC3/IR images, showing the BCG in A2261 and its neighbors in the central 2 × 2 arcmin region of the cluster. The inset in the lower right-hand corner shows a zoomed-in region centered on the BCG with contrast adjusted to highlight the bright knots (labeled 1, 2, 3, 4) in the core. The orientation is north up and west to the right. The faint "figure 8" patterns at the 6 o'clock and 11 o'clock positions are due to internal reflections in the ACS camera of light from a nearby bright star. The red "diamond" at the 10 o'clock position near the BCG is caused by a gap in areal coverage due to the multiple orientations used in the CLASH survey. The red "blob" at the right edge of the image is a WFC3/IR detector artifact that does not easily calibrate out.

If the radio source is at the cluster redshift then the FIRST detection yields an absolute luminosity of 7.8×10^{39} erg s^{-1} at 1.4 GHz corresponding to $L_{1.4\,\mathrm{GHz}} = 5 \times 10^{23}$ W Hz^{-1}. Hlavacek-Larrondo et al. (2012) also find a central source with luminosity 5.0×10^{39} erg s^{-1} at 5 GHz corresponding to $L_{5.0\,\mathrm{GHz}} = 1 \times 10^{23}$ W Hz^{-1}. The radio fluxes are indicative of a mildly powerful FR I radio source typical of those seen in BCGs (e.g., Croft et al. 2007)

Apart from the radio source, there is also a faint 24 μm detection of 0.44 mJy (Hoffer et al. 2012), which would indicate either star formation or a hot dust torus around an AGN. As in the case of the radio observations, however, the angular resolution is probably too poor to distinguish whether or not the flux comes from the center of the core or any of the associated knots.

In contrast, optical spectra do not reveal any significant evidence of emission lines that may be associated with an AGN or cooling flow activity (the spectra are presented in the next subsection). Further, there are no known X-ray or EUV sources identified with any of the compact knots; the X-ray limit on any point source in the core is $L_{2-10\,\mathrm{keV}} < 3.8 \times 10^{41}$ erg s^{-1} (Hlavacek-Larrondo et al. 2012). At the same time, it is typical for central radio source in BCGs not to have strong X-ray counterparts. A black hole mass of $\sim 10^{10}\,M_{\odot}$ is in general consistent with the power requirements associated with the ICM shock fronts seen in other clusters (e.g., McNamara et al. 2009); but for such high-mass black holes, the power needed for such shocks is only $\sim 0.001 L/L_{\mathrm{ed}}$, which therefore implies that the black holes can be radiatively inefficient. Hlavacek-Larrondo et al. (2012) note that synchrotron cooling can strongly affect the X-ray luminosity from the most massive black holes since the cooling break occurs below X-ray wavelengths, making such massive black holes underluminous at X-ray wavelengths compared to their radio luminosity. For A2261-BCG in particular, Hlavacek-Larrondo et al. (2012) estimate an Eddington ratio of $\sim 10^{-6}$–10^{-8}.

2.2. Photometry

The details of the image reduction and co-addition of the A2261 *HST* observations are given in Postman et al. (2012) and Coe et al. (2012). The analyses of the BCG profile here are based on the F606W and F814W *HST* CLASH images. The Advanced Camera for Surveys (ACS) photometry is on the AB magnitude system but we will express much of the reduced photometry in the rest-frame V band (Vega-based) for compatibility with the Lauer et al. (2007a) analysis of central galaxy photometry. We use a suite of Bruzual & Charlot (2003, hereafter BC03)

Table 1
A2261 BCG and Bright Knot Astrometry and Photometry

Object ID	R.A. (J2000)	Decl. (J2000)	F814W (AB mag)[a]	F606W–F814W (AB mag)[a]	V mag (Vega mag)[b]	M_V (Vega mag)[c]
BCG	17:22:27.18	+32:07:57.30	14.69	0.82	15.53	−24.70
			(<0.01)	(<0.01)	(0.01)	(0.02)
Knot 1	17:22:27.23	+32:07:57.65	21.53	0.86	22.15	−17.85
			(0.02)	(0.04)	(0.06)	(0.06)
Knot 2	17:22:27.21	+32:07:57.56	21.89	0.85	22.50	−17.49
			(0.02)	(0.04)	(0.06)	(0.06)
Knot 3	17:22:27.13	+32:07:57.59	20.20	0.83	20.80	−19.20
			(0.02)	(0.04)	(0.06)	(0.06)
Knot 4	17:22:27.14	+32:07:55.85	22.93	0.97	23.61	−16.63
			(0.02)	(0.04)	(0.06)	(0.06)

Notes. [a] Corrected only for Galactic extinction.
[b] Corrected for Galactic extinction and K-dimming (assuming sources are at the cluster redshift).
[c] Corrected for Galactic extinction, K-dimming, and passive evolution from $z = 0.224$ to $z = 0$. See the text for details.

synthetic stellar population models to derive linear photometric transformations from the observed, extinction-corrected ACS/WFC magnitudes and colors to the rest-frame Johnson V band, V_o. The BC03 models used to empirically derive the transformation equations have the following parameters: exponential star formation rate e-folding times, τ, of 0 Gyr (SSP model), 0.2 Gyr, 0.6 Gyr, and 1.0 Gyr; metallicities of 0.25 $Z_\odot$, 1.0 $Z_\odot$, and 2.5 $Z_\odot$; and ages from 2 Gyr to the age of the universe at the cluster redshift in 0.5 Gyr intervals. These models more than span the range of observed cluster galaxy spectral energy distributions (SEDs). To compute photometric transformations, we take the BC03 SEDs for each of the above models and compute the observed photometry and colors at the cluster redshift and then use the same SEDs to compute the rest-frame Johnson V magnitude. The transformation equation parameters are then derived using a linear least-squares fitting procedure. In addition, we compute an evolution correction, $c_{\rm ev}$, from a BC03 $\tau = 0.6$ Gyr solar metallicity model with a formation epoch of $z = 4.5$. The transformation equation is

$$\begin{aligned} V_o &= ({\rm F814W} + c_{\rm ev,F814W}) + 0.5186 \\ &\quad \times ({\rm F606W} - {\rm F814W} + c_{\rm ev,F606W} - c_{\rm ev,F814W}) + 0.1764 \\ &= ({\rm F814W}) + 0.5186 \times ({\rm F606W} - {\rm F814W}) + 0.4213, \quad (1) \end{aligned}$$

where F606W and F814W are the Galactic extinction-corrected ACS/WFC measurements in AB-magnitudes, $c_{\rm ev,F606W} = 0.256$, $c_{\rm ev,F814W} = 0.233$, and V_o is on the Vega system. The extinction corrections used are 0.127 mag and 0.079 mag for the F606W and F814W filters, respectively. The rms scatter about the transformation equation shown in Equation (1) is 0.006 mag. We tested the robustness of the method by computing similar transformations for F625W and (F625W–F814W) and for F850LP and (F814W–F850LP). They yield the same rest-frame V_o values to within ±0.01 magnitudes.

The total luminosity of A2261-BCG was determined by fitting its surface photometry with an $r^{1/4}$ law. This is consistent with the methodology in Lauer et al. (2007a), which will be used to provide the context for the present galaxy. The BCG is highly luminous with a total absolute magnitude of −24.70 in the V band (see Table 1). Because we want to compare this to the $z = 0$ sample of BCGs, this luminosity includes an evolutionary correction of +0.26 mag to account for the aging of the stellar population since the $z = 0.22$ epoch. Even then, A2261-BCG is among the most luminous BCGs known (Postman & Lauer 1995).

Four sources fall within the outskirts of the core. Their coordinates and photometric properties are summarized in Table 1. The brightest source, "Knot 3," is well resolved. Its profile was measured simultaneously with the BCG (as is described in Section 3.1) and has a roughly exponential form. The close pair of compact sources northeast of the core center, Knots 1 and 2, are both marginally resolved with 0.″05 half-intensity radii. The faint source south of the core, Knot 4, is unresolved. The photometric errors in Table 1 given here include both the random and estimated systematic errors. The random errors (photon shot noise, read noise, dark current) are in the range 0.005–0.010 mag. The systematic errors are relatively small but still about 2–4 times larger than the corresponding random errors. This is due to spatial variations in the background level after the BCG model is subtracted from the image. To estimate the amplitude of the systematic error we compared the knot photometry derived from the BCG-subtracted image with that derived by using a local sky subtraction (instead of BCG subtraction) where the background is estimated from an annulus with an inner radius of 0.″6 and an outer radius of 1.″2 centered on each knot. The two measures of the photometry typically agree to within 0.015–0.020 mag. Based on this, we adopt 0.018 mag as an estimate of the systematic error.

2.3. Spectroscopy and the Central BCG Velocity Dispersion

Moderate resolution spectroscopy of the BCG exists from the Sloan Digital Sky Survey (SDSS) DR8 and from the Gemini Observatory data archive. The Gemini data are deep long-slit spectra with GMOS-N from the program GN-2008A-Q-103 (PI: Chris Bildfell). The A2261 observations were obtained on 2008 March 16. The GMOS-N long-slit, with 0.″75 width, was placed on the BCG and oriented at a position angle that intersects two of the three bright knots in the northern part of the core (but not the brightest one). The spectra are split into dual red and blue channels to optimize sensitivity. The full spectral range is ∼4140–6040 Å with a spectral resolution of $R \sim 1000$ at the blue end. The one-dimensional co-added GMOS spectrum is shown in Figure 2.

We measured the stellar velocity dispersion (σ) within the core of A2261-BCG from the GMOS spectrum using the IDL code pPXF developed by Cappellari & Emsellem (2004), which fits a linear combination of template spectra to the observed galaxy spectrum to minimize template mismatch. The template spectra are provided by the Vazdekis et al. (2010) single burst

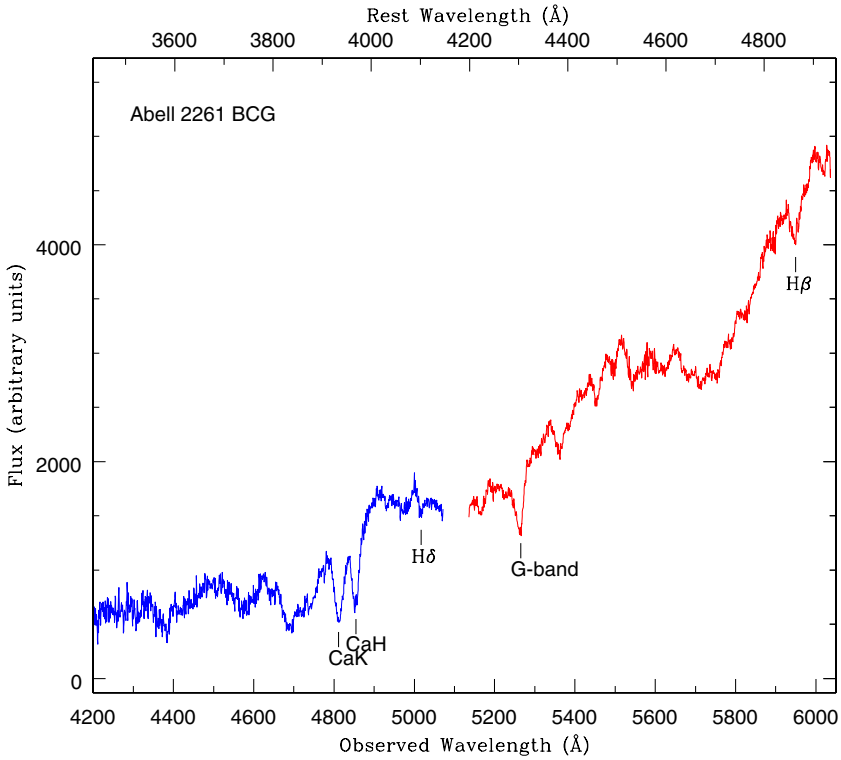

Figure 2. Spectrum of the BCG in A2261. Its redshift is $z = 0.2232$. This spectrum is from the GMOS spectrograph on the Gemini-N 8 m telescope (PI: H. Hoekstra). Prominent absorption features are noted. The data from the GMOS blue and red channels are denoted, respectively, by the blue and red traces. The break at 5100 Å is due to a small data gap between the two channels. This spectrum was used to derive the stellar velocity dispersion of the BCG reported in this work, $\sigma = 387 \pm 16$ km s^{-1}.

(A color version of this figure is available in the online journal.)

models for a range of ages and metallicities, which are based on the empirical MILES stellar library (Sánchez-Blázquez et al. 2006).

The fits are computed separately in the red and blue channel spectra, covering rest-frame wavelengths 3700–4150 Å and 4250–4700 Å, respectively in order to avoid regions near the chip edges where the wavelength solution is less reliable. The bright skyline at the 5682–5688 Å Na doublet is masked in the fitting procedure, and the fits are computed weighting all pixels equally. We find consistent values of $\sigma = 393 \pm 13$ km s^{-1} on the blue side and $\sigma = 380 \pm 8$ km s^{-1} on the red side. The higher-order non-Gaussian velocity moments $H3$ and $H4$ derived from the fits are negligible. We therefore adopt $\sigma = 387 \pm 16$ km s^{-1} as an estimate of the ensemble stellar velocity dispersion, including systematic errors. The Gemini velocity dispersion value is in excellent agreement with the 388 ± 19 km s^{-1} velocity dispersion estimate from the DR8 SDSS database. This is among the highest central velocity dispersion values known.

3. THE CENTRAL STRUCTURE OF A2261-BCG

3.1. The Morphology of the Core

The surface brightness profile of A2261-BCG was measured from the F814W image deconvolved with 20 cycles of Lucy (1974)–Richardson (1972) deconvolution to correct for the blurring of the point spread function (PSF). The deconvolved image of the core is given in Figure 3. Deconvolution works well on *HST* images for recovering estimates of the intrinsic light distributions of galaxies (Lauer et al. 1998, 2005). Given the angularly large and flat profile of the A2261-BCG core, the effects of deconvolution in the present context are extremely modest. The increase in the central surface brightness within the core after deconvolution is only ∼3%, with similar effect on the measured angular size of the core. The real import of deconvolution for A2261-BCG is to recover the forms of the compact sources falling around the core, and to reduce the effects of their scattering "wings" on the core, itself.

Figure 3 also shows the residuals obtained after a two-dimensional model reconstructed from the brightness profile of the core was subtracted from the image. The profile for $r > 0\farcs5$ was measured using the Lauer (1986) algorithm (operating in the `xvista` image processing system), which solves for the overlapping light distributions of multiple galaxies; the high-resolution algorithm of Lauer (1985) was used interior to this. The surface brightness profile is presented in Figure 5. The profile ratifies the visual impression that the core is essentially flat. In contrast to the typical central structure of most elliptical galaxies (but not all; see Lauer et al. 2002), there is no sign of any rising cusp in starlight as $r \to 0$. The lack of a cusp actually made it difficult to determine the precise center of the galaxy. We did this by taking an intensity centroid over the entire core.

At radii well outside the core, *HST*-based surface brightness profiles become vulnerable to systematic sky measurement errors and so on due to the low-intensity levels of the outer isophotes, the angularly small pixels, and limited fields of the cameras. To better characterize the envelope of A2261-BCG, we augmented the ACS photometry with surface photometry measured from a ground-based *R*-band image obtained with the Suprime-Cam imager on the Subaru 8 m telescope. The Subaru-derived profile was scaled to match the ACS profile over $5'' < r < 8''$, then blended with it over the same interval, and used solely as the brightness distribution for $r > 8''$. The

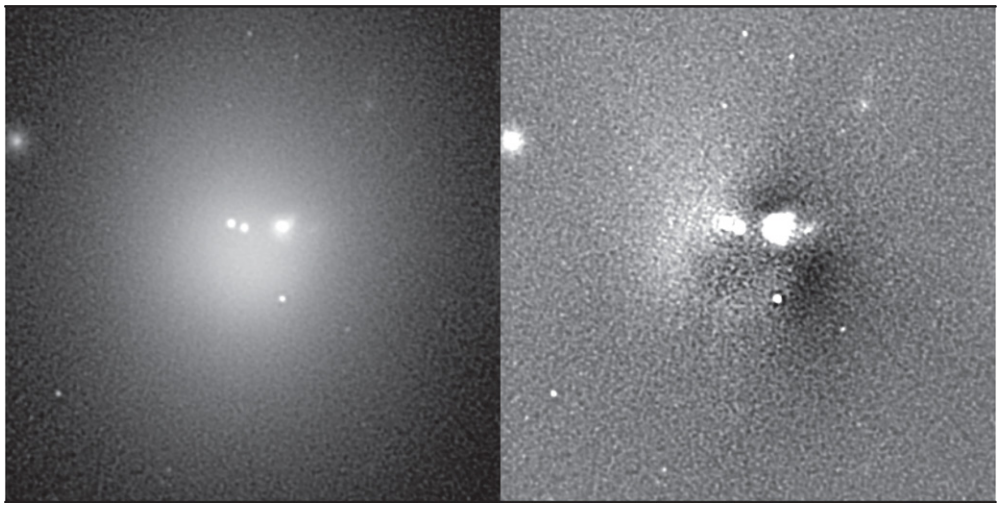

Figure 3. The left panel shows the center of the F814W image of the BCG after Lucy (1974)–Richardson (1972) deconvolution. The region shown is $12'' \times 12''$ (43.2×43.2 kpc); the intensity scale is logarithmic. North is at the top and east to the left. The right panel shows the residuals after subtraction of a model reconstructed from the surface photometry of the BCG. The overall structure of the residuals is a dipole pattern of positive residuals NE of the core and negative residuals to the SW. This suggests that the core is slightly displaced from the surrounding envelope in the SW direction.

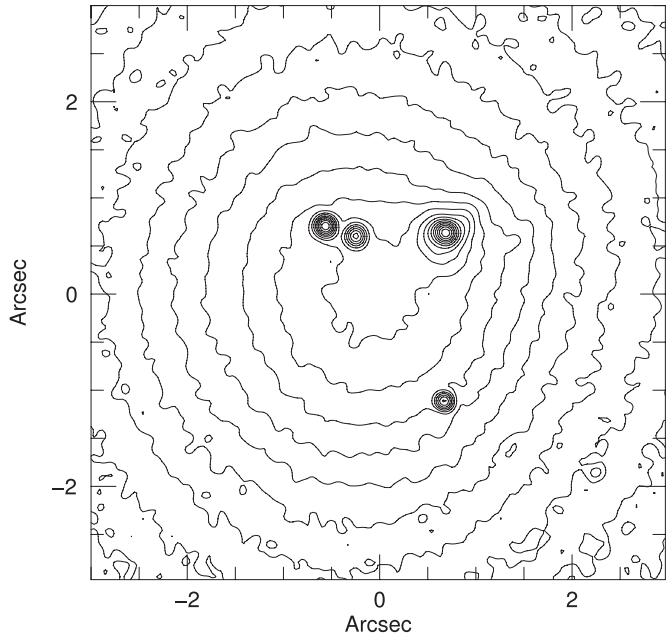

Figure 4. Contour plot of the core of A2261-BCG. The contour levels have an arbitrary zero point, but are spaced by 0.25 mag in surface brightness. North is to the top and east to the left. Note that the contour levels are closer together in the SW direction outside the core than they are in the NE, supporting the dipole-like residual pattern seen in Figure 3 and the conclusion that the core is displaced to the SW relative to the envelope center.

Subaru profile extends to $\sim 24''$ and equivalent V-band surface brightnesses fainter than 25 mag arcsec^{-2}.

Despite the smooth structure of the profile, the residuals within the core show a number of interesting features. In addition to the presence of the four sources noted earlier, the residuals show a dipole-like pattern outside the central flat portion of the profile. The simplest interpretation is that the core is slightly displaced from the center of the surrounding envelope by $\sim 0\farcs2$ (0.7 kpc) toward position angle $\sim 300^\circ$. This conclusion is supported by the contour map of the core, shown in Figure 4. The contour lines outside of the core to the SW are clearly spaced closer together than those in the NE direction.

3.2. Analysis of the Surface Brightness Profile

We describe the profile with a "Nuker law" (Lauer et al. 1995),

$$I(r) = 2^{(\beta-\gamma)/\alpha} I_b \left(\frac{r_b}{r}\right)^{\gamma} \left[1 + \left(\frac{r}{r_b}\right)^{\alpha}\right]^{(\gamma-\beta)/\alpha}, \qquad (2)$$

which models the surface brightness distribution as a "broken" power law. The envelope profile has the form $I(r) \sim r^{-\beta}$ as $r \rightarrow \infty$, while the inner cusp has $I(r) \sim r^{-\gamma}$ as $r \rightarrow 0$, with the transition radial scale provided by the "break radius," r_b. The "speed" of transition between the envelope and inner cusp is provided by α, while I_b, the surface brightness at r_b gives the overall intensity normalization.

The best-fitting Nuker law is plotted in Figure 5 and has the parameters $\gamma = -0.01, \beta = 1.56$, $\alpha = 2.41 \pm 0.18, r_b = 1\farcs20$, and I_b of 19.72 in F814W(AB). The fit was conducted for $r < 8''$, beyond which the envelope falls away slightly faster than a pure power law with radius. As can be seen, the fit over this domain is excellent, with an rms residual of 0.02 mag. The parameters are not strongly dependent on the domain of the profile fitted, in any case. For a fit conducted limited to $r < 3\farcs7$, or half of the nominal domain, $r_b = 1\farcs15$ is recovered, only a 4% decrease from the nominal value. The break radius, r_b, corresponds to the point of maximum logarithmic curvature, and thus can also be estimated by non-parametric methods. Lauer et al. (2007a) did this for a large sample of core galaxies presented in Lauer et al. (2005), finding the Nuker-fit and non-parametric measurements to agree well over a large range in angular core size, with no biases.

The negative γ actually implies that the surface brightness decreases slightly as $r \rightarrow 0$. We also performed a Nuker fit forcing $\gamma = 0$, which is essentially identical to the nominal fit, but for the central point. In this case, we recover $\beta = 1.55$, $\alpha = 2.50, r_b = 1\farcs30$, and I_b of 19.72. The $\gamma = 0$ model falls right on the upper error bar of the central point and thus coincidentally serves as a 1σ confidence bound on the central profile.

The center of A2261-BCG may have a luminosity *density* profile that actually decreases as $r \rightarrow 0$. This occurs in a number of galaxies including a few BCGs (Lauer et al. 2002, 2005).

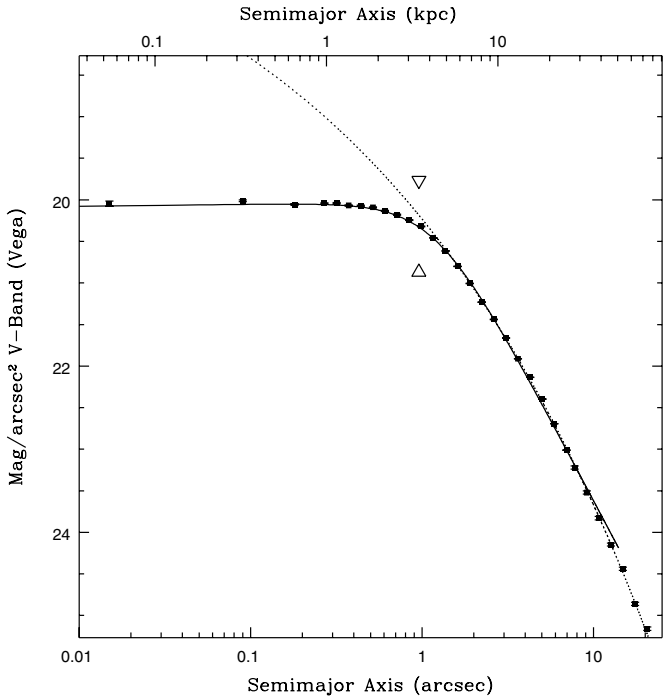

Figure 5. Central surface brightness profile of A2261-BCG as measured (solid points) is shown with two "Nuker-law" profile fits (Lauer et al. 1995). The error bars are smaller than the points, but for the central few measurements. For comparison to previous studies the profile is normalized to $z = 0$ V band (Vega). The solid line is the best-fitting Nuker law and features a slightly depressed ($\gamma = -0.01$) cusp as $r \rightarrow 0$. The dotted line is an $r^{1/4}$ law (an $n = 4$ Sérsic law) fitted to the envelope. The triangles indicate the cusp radius.

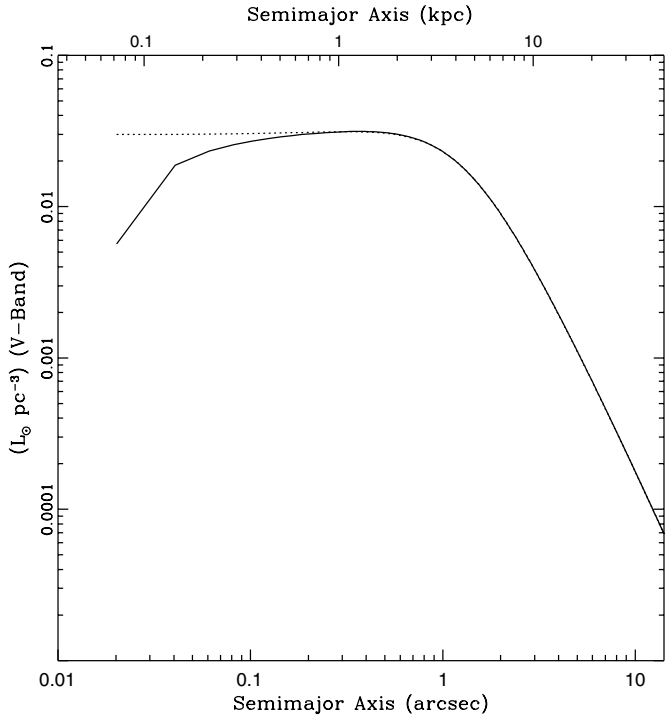

Figure 6. Implied luminosity density profile of A2261-BCG. The density profile resulting from Abel inversion of the best-fitting Nuker law, which features a slightly depressed ($\gamma = -0.01$) cusp as $r \rightarrow 0$, is shown as a solid line. The density profile plotted as a dotted-line is based on inversion of a Nuker law fitted with $\gamma = 0$. The small difference between the two profiles is greatly amplified in density as $r \rightarrow 0$. Even the density profile with $\gamma = 0$ is formally very slightly depressed as $r \rightarrow 0$. The difference between the two models is not significant.

An Abel inversion of the Nuker model for A2261-BCG with $\gamma = -0.01$ indeed shows that $r = 0$ corresponds to a local minimum in stellar density (Figure 6). Even inversion of the $\gamma = 0$ model of the brightness profile formally implies a ~4% decrease in luminosity density at the *HST* resolution limit. This can be understood as a consequence of the lack of a cusp in combination with a sharply defined core. With a generic surface brightness profile of the form $I(r) \propto (1 + r^{\alpha})^{-\beta/\alpha}$ (both α and β positive), the derivative of the profile has the form $I(r)' \propto r^{\alpha}$ for $r \ll 1$. When used with the standard Abel transform, this implies a formal density of zero at $r = 0$, when $\alpha > 2$, a condition satisfied for the A2261-BCG brightness profile.

Given, however, the modest central decrease in density implied by even the $\gamma = -0.01$ model, which just occurs near the resolution limit, it is not possible to say with confidence if A2261-BCG is yet another example of a "hollow core." At the same time there is no sign of any centrally *rising* cusp in central surface brightness, and an even *constant* density core over nearly two decades in radius is unusual (see the collection of core density profiles in Lauer et al. 2007b).

3.3. The A2261-BCG Core Compared to Those of Other Early-type Galaxies

Figure 7 shows that the core of A2261-BCG is the largest core yet seen among extensive surveys of local galaxies. The figure is an adaptation of a figure in Lauer et al. (2007a), which shows the relationship between the core "cusp radius," r_{γ}, and the total V-band luminosity, L_V, for a composite sample of *HST* studies of the central structure of early-type galaxies (Lauer et al. 1995, 2005; Faber et al. 1997; Quillen et al. 2000; Ravindranath et al.

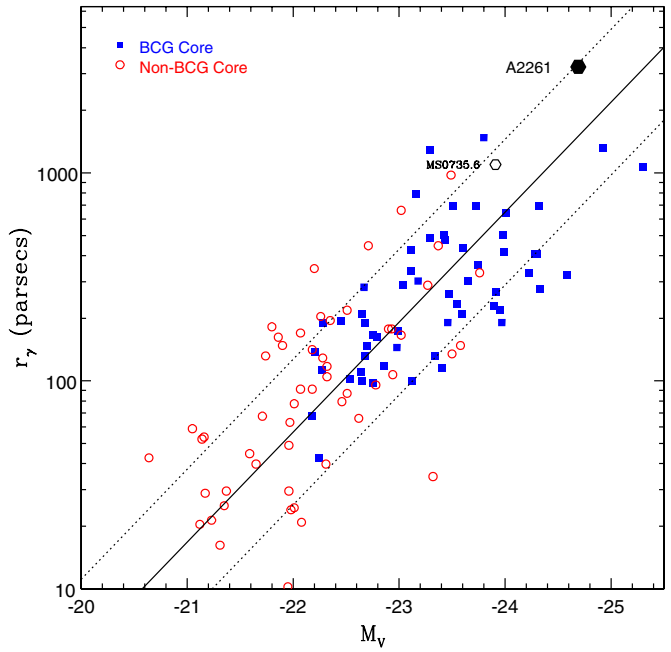

Figure 7. Relationship between cusp radius and total galaxy luminosity (V-band Vega-based). The galaxy sample plotted was assembled in Lauer et al. (2007a) from a variety of sources (the figure is adopted from Figure 5 in that paper). The BCGs in particular come from the Laine et al. (2002) sample. The Lauer et al. (2007a) $r_{\gamma} - L$ relationship (also given in Equation (4)) is plotted; the dotted lines indicate $\pm 1\sigma$ scatter about the mean relationship. A2261-BCG is plotted at the top, clearly has a cusp radius larger than all other galaxies in the sample. The large core in the MS0735.6+7421 BCG discovered by McNamara et al. (2009) is also plotted for comparison.

(A color version of this figure is available in the online journal.)

2001; Rest et al. 2001; Laine et al. 2002).[15] The Laine et al. (2002) study, in particular, is focused on the central structure of BCGs and is thus particularly useful for placing the core of A2261-BCG in context.

The cusp radius is the angular or physical scale at which the local logarithmic slope of the surface brightness profile reaches a value of $-1/2$, as the profile transitions from the steep envelope to the shallower inner cusp. In terms of the Nuker-law parameters,

$$r_\gamma \equiv r_b \left(\frac{1/2 - \gamma}{\beta - 1/2} \right)^{1/\alpha}. \quad (3)$$

This scale was first introduced by Carollo et al. (1997) and adopted in the analysis of Lauer et al. (2007a), who demonstrated that it gave tighter relationships between the core and global properties of the galaxies than the direct use of the break radius, r_b, did.

For A2261-BCG, the $\gamma = -0.01$ Nuker-law fit yields $r_\gamma = 0\farcs89 \pm 0\farcs02$ or 3.2 ± 0.1 kpc at the distance of A2261-BCG (the $\gamma = 0$ fit also gives $r_\gamma = 0\farcs89$). As a check, this value is consistent with a simple estimate of $r_\gamma = 0\farcs90$, made by fitting a parabola to the core over $0\farcs7 < r < 1\farcs4$. The corresponding "cusp brightness," I_γ, the surface brightness at r_γ, is 19.52 mag arcsec^{-2} (F814W) or 20.29 in the rest-frame V band corrected for interstellar extinction. As shown in Figure 7, this r_γ is over twice as large as the largest BCG cores seen in the Laine et al. (2002) sample. It is also three times larger than the large core in MS0735.6+7421-BCG noted by McNamara et al. (2009). The A2261-BCG core falls on the high side of the Lauer et al. (2007a) relation between core size and total galaxy luminosity,

$$\log(r_\gamma/\mathrm{pc}) = (1.32 \pm 0.11)(-M_V - 23)/2.5 + 2.28 \pm 0.04. \quad (4)$$

The scatter in $\log(r_\gamma)$ about this relation is 0.35 dex; A2261-BCG falls 0.33 dex above the relation, corresponding to a 1.0σ deviation.

4. CONJECTURES ABOUT SUPERMASSIVE BLACK HOLES IN THE CORE

4.1. Estimates of the Black Hole Mass from the Core Size

If cores are created by the scouring action of a binary black hole, and the core size is indicative of the mass of the binary, then the implied black hole mass for A2261-BCG must be extremely large. McConnell et al. (2011) recently identified two black holes with masses $10^{10}\,M_\odot$ or greater in the BCGs A1367-BCG (= NGC 3842) and A1656-BCG (= NGC 4889), which have cusp radii of only 0.3 kpc and 0.7 kpc, respectively (Lauer et al. 2007a), implying that $M_\bullet$ in A2261-BCG is yet larger than that found in those two galaxies.

The $M_\bullet$–L and $M_\bullet$–σ relations between nuclear black hole mass and galaxy luminosity (Dressler 1989; Kormendy & Richstone 1995; Magorrian et al. 1998) or velocity dispersion (Ferrarese & Merritt 2000; Gebhardt et al. 2000) give some guidance on what to expect for the central black hole mass in A2261-BCG, completely apart from its core structure. The $M_\bullet$–L and $M_\bullet$–σ (elliptical galaxy only sample) relations from the comprehensive analysis of Gültekin et al. (2009) predict $M_\bullet = 6 \times 10^9\,M_\odot$ and $2 \times 10^9\,M_\odot$, respectively. The analogous McConnell et al. (2011) $M_\bullet$–L and $M_\bullet$–σ relations, which as noted above include BCG black hole masses, predict somewhat higher values of $1.1 \times 10^{10}\,M_\odot$ and $5 \times 10^9\,M_\odot$. It should be noted that A2261-BCG is more luminous and has a higher velocity dispersion than any galaxy that actually has a black hole mass measurement, thus the predictions are extrapolations.

A different approach is to use the fundamental plane of black hole activity (Merloni et al. 2003), which derives $M_\bullet$ from a combination of 5 GHz core radio luminosity and 2–10 keV nuclear X-ray emission. Hlavacek-Larrondo et al. (2012) use this methodology to estimate $M_\bullet = 2.0^{+8.0}_{-1.6} \times 10^{10}\,M_\odot$ for A2261-BCG.

Unfortunately, estimates of black hole mass implied by the scale of the core, itself, in A2261-BCG will be even more uncertain extrapolations. Lauer et al. (2007a) presented a number of relationships between r_γ and $M_\bullet$, based on how the sample of core galaxies with real $M_\bullet$ determinations was analyzed. If r_γ and $M_\bullet$ are fitted symmetrically, then Lauer et al. (2007a) find $r_\gamma \propto M_\bullet^{0.8}$, which predicts $M_\bullet \sim 4 \times 10^{10}\,M_\odot$ for A2261-BCG. If on the other hand $M_\bullet$ is treated as an independent variable, then Lauer et al. (2007a) find $r_\gamma \propto M_\bullet^{1.5}$, which predicts a more modest $M_\bullet \sim 7 \times 10^9\,M_\odot$. The large difference between the two estimates is due to the small number of systems contributing to the Lauer et al. (2007a) r_γ–$M_\bullet$ relationships and the large scatter between the two parameters.

An alternate approach advocated in several papers is to relate estimates of the "mass deficit," M_d, that is the mass in stars that was ejected to generate the core, to $M_\bullet$. Unfortunately, this methodology at present also leads to large uncertainties in the estimated $M_\bullet$ for A2261-BCG. Kormendy & Bender (2009) derive a relationship between L_d and $M_\bullet$ for galaxies of the form $L_d \propto M_\bullet$, where L_d is the observed *starlight* rather than inferred mass deficit, and is measured by integrating the central difference between the observed surface brightness profile and an inward extrapolation of a Sérsic law fitted to the envelope of the galaxy.

The best fit of a Sérsic law to the envelope of A2261-BCG has $n = 4.1$, or essentially the classic $r^{1/4}$ law form. An $r^{1/4}$ law fitted to the envelope gives $M_V \approx -20.8$, implying $M_\bullet \sim 1.1 \times 10^{10}\,M_\odot$, using the Kormendy & Bender (2009) relation. This later L_d is identical to $M_V \approx -20.8$ derived by the simple estimate of "core luminosity," $L_\gamma \equiv \pi I_\gamma r_\gamma^2$ used by Lauer et al. (2007a) as a proxy for L_d that avoids the need for the careful selection and evaluation of a "pre-scouring" reference surface brightness profile.

4.2. Ejection of the Central Black Hole

One intriguing possibility is that the large flat core has resulted from the central ejection of its nuclear black hole. In this scenario, the galaxy most likely had a large core to begin with, which would have been enlarged by the ejection of the central black hole. The large core would have been generated by a smaller black hole than that directly implied by the presumption that scouring by the binary black hole did all the work.

Merritt et al. (2004) and Boylan-Kolchin et al. (2004) show that a core can be generated directly in a "power-law" galaxy (a system that initially has a steep central cusp) when the components of a binary black hole merge and the remnant is ejected by the asymmetric emission of gravitational radiation. Gualandris & Merritt (2008) simulated this scenario, finding that the ejection can substantially enlarge a pre-existing core, leading to the inference of an exceptionally large mass deficit. Given the high luminosity of A2261-BCG, it is extremely likely

[15] The V band used in Lauer et al. (2007a) and cited in the remainder of the paper is Vega-based.

that it would have a large core prior to any ejection of a central black hole. Gualandris & Merritt (2008) also show that the central stellar density profiles can become extremely flat after ejection of the black hole, similar to what is seen in Figure 6.

The physical displacement of the core from the envelope center, noted above, is indicative of a local dynamical disturbance. This is likely to be a relatively recent event. An ejected black hole would be trailed by a strong dynamical-friction wake as it leaves the core. In effect, it would "pluck" the core, which would then oscillate for a few crossing times, $t_c \sim r_\gamma/\sigma$ or $\sim 10^7$ yr for A2261-BCG. At the same time, this need not mean that the ejection of the black hole, itself, needs to be as recent. If the ejected black hole remains on a radial orbit that periodically returns to the core, then the disturbance might only be due to a recent passage (D. Merritt 2012, private communication).

Real proof of the ejected black hole hypothesis would be to find direct evidence of the ejected black hole, itself. Merritt et al. (2009) show that the ejected black hole carries along with it a "cloak" of stars that had previously been closely bound to it. The ejected black hole and associated stars would somewhat resemble a globular cluster or ultracompact dwarf galaxy. The key diagnostic for such a system would be the extremely high velocity dispersion of the tightly bound stars. An obvious question then for the present case is if any of the four sources proximal to the core might be such an object.

An important point is that the stellar "cloak" is most likely to be considerably less massive than the black hole. For a black hole ejected from a core, Merritt et al. (2009) find

$$\frac{M_b}{M_\bullet} \approx 2 \times 10^{-2} \left(\frac{\sigma}{200\ \mathrm{km\ s^{-1}}}\right)^{5/2} \left(\frac{V_k}{10^3\ \mathrm{km\ s^{-1}}}\right)^{-5/2}, \quad (5)$$

where M_b is the mass of stars bound to the black hole, σ is the velocity dispersion of the galaxy, and V_k is the "kick" velocity with which the newly merged binary black hole is ejected from the center of the galaxy. In the case of A2261-BCG with $\sigma = 387\ \mathrm{km\ s^{-1}}$, the coefficient in the above equation becomes 0.1. While we have echoed the nominal $V_k = 1000\ \mathrm{km\ s^{-1}}$ from Merritt et al. (2009), the real value depends on the unknown mass ratio and spins of the two black holes within the merging binary and can range from essentially zero to a few thousand km s^{-1}. The only way to constrain V_k better would be to identify the remnant and measure its line-of-sight velocity.

Merritt et al. (2009) also show that the effective radius of the cloak is also related to the kick velocity. For a black hole initially in a core,

$$R_e \approx 43 \left(\frac{M_\bullet}{10^{10}\ M_\odot}\right) \left(\frac{V_k}{10^3\ \mathrm{km\ s^{-1}}}\right)^{-2} \mathrm{pc}. \quad (6)$$

Given the expected scale and mass of the stellar cloak, the best candidate for an ejected black hole would be the least luminous of the four sources, the unresolved point source south of the core. The most luminous of the four sources has an implied luminosity of $L_V \sim 4 \times 10^9\ L_\odot$ and a substantially larger physical extent than the number given above. When converted to a likely mass, the source carries a substantial fraction of the putative $10^{10}\ M_\odot$ black hole, thus not matching the expectation that $M_b \ll M_\bullet$. Morphologically, the source also resembles any number of other small galaxies visible within the neighborhood of the BCG. The two less luminous paired-sources, also north of the core, are more consistent with a possible cloak, but even their compact sizes are large for the expectations enumerated above.

Of course if V_k is large, and the ejection happened long ago, then the remnant would be unlikely to be within the core, and the candidate list would have to be extended to sources at much larger distances from the center of the BCG. The timescale for exiting the core is simply r_γ/V_k, which is likely to be substantially shorter than t_c. Conversely, a small kick favors larger and more extended cloaks, and increases the likelihood that the remnant would remain close to the core in the event that the kick was insufficient to unbind the black hole from the BCG, itself. If the offset core is indeed due to an ejected black hole, then the short lifetime of the offset would imply that the remnant should be relatively close-by.

5. A2261-BCG AND THE FORMATION OF CORES

There is a rich tradition in observational astrophysics of using the extreme member of an ensemble to understand the origin of the ensemble over all. The role of A2261-BCG as a witness to the mechanisms that form cores hinges on whether its core is "normal" or not. A2261-BCG bests its closest rival, NGC 6166, for having the largest core by a factor of two. More generally, the core of A2261-BCG stands out from all galaxies in the subset of 57 BCGs in the Lauer et al. (2007a) composite sample of early-type galaxies imaged with *HST* (the great majority of the BCGs were provided by Laine et al. 2002). Still, the core $r_\gamma = 3.2$ kpc does not fall far above the Lauer et al. (2007a) r_γ–L relationship, given that A2261-BCG also has an unusually large total luminosity—even as compared to other BCGs. A2261-BCG might be expected to harbor a $\sim 10^{10}\ M_\odot$ black hole, based on its location within the $M_\bullet$–L and $M_\bullet$–σ relations, thus the formation of core in this galaxy would a priori be expected to a limiting case for the formation of the core by core scouring, the standard hypothesis.

The core of A2261-BCG was not at first noted for its size, as much as its unusual appearance, however. Cores generally have at least a weak central surface brightness cusp, but in A2261-BCG there is no obvious center to the core. Its central stellar density profile is perfectly flat, or perhaps even depressed at the center. While there is a radio source coincident with the core, there is no optical AGN counterpart or central nuclear star cluster—nothing suggests that A2261-BCG is hosting anything like a $\sim 10^{10}\ M_\odot$ black hole at its center. If binary black holes do scour out cores, then on occasion they must also merge and be ejected from the core, thus causing it to rebound and expand to an even larger size than it possessed at the completion of scouring. An attractive feature of this scenario is that it may account for large cores that may be difficult to explain by scouring alone. The simulations of Merritt et al. (2004), Boylan-Kolchin et al. (2004), and Gualandris & Merritt (2008) suggest that the core of A2261-BCG matches the expectations of what a core that has ejected its central black hole looks like.

There is a caveat, however. Cores with ejected black holes may be ephemeral. Faber et al. (1997) note that a central black hole can act as "guardian," "protecting" an existing core from being infilled by the central cannibalism of less luminous, but centrally denser galaxies. A2261-BCG lives in a rich environment. Figure 6 shows that the central mass density of the core is $<0.1\ M_\odot\ \mathrm{pc}^{-3}$, which is extremely diffuse in comparison to the denser cores of less luminous galaxies. Without a central black hole in the core of A2261-BCG, the nuclei of galaxies merging with the BCG would readily settle intact into its center (Holley-Bockelmann & Richstone 2000). The four sources projected against the core are a reminder that the galaxy may cannibalize its neighbors, even if the sources

in question may themselves not be at risk for this. Again, if A2261-BCG did lose its central black hole, this may have been a relatively recent event.

In the end, how we use A2261-BCG to test the theory of core formation hinges on whether or not it now hosts a supermassive black hole at its center. The radius interior to which a black hole dominates the stellar dynamics is $r_\bullet \equiv GM_\bullet/\sigma^2$. For a $\sim 10^{10}\,M_\odot$ black hole and $\sigma = 387$ km s^{-1}, $r_\bullet \approx 300$ pc or $\approx 0\farcs08$ for A2261-BCG. This scale is readily accessible using adaptive optics in the near-IR on 10 m class telescopes, with the caveat that the extremely low surface brightness interior to the core will demand long exposures, even with such large apertures. The detection of a *central* $M_\bullet \sim 10^{10}\,M_\odot$ would suggest that the core is simply an extreme example of the scouring mechanism. Conversely, a demonstration that A2261-BCG lacks a suitably massive black hole, or the possible demonstration that one of the sources near the core is a cloaked black hole could establish that the large core indeed was generated by the ejection of its central black hole. An improved position for the central radio source might also determine if a black hole truly lies at the center of the core, or instead is associated with one of the knots.

We thank David Merritt for useful conversations. Based on observations made with the NASA/ESA *Hubble Space Telescope*, obtained at the Space Telescope Science Institute, which is operated by the Association of Universities for Research in Astronomy, Inc. (AURA), under NASA contract NAS 5-26555. The *HST* observations are associated with GO proposal 12066. Also based on observations obtained at the Gemini Observatory (acquired through the Gemini Science Archive), which is operated by the AURA under a cooperative agreement with the NSF on behalf of the Gemini partnership: the National Science Foundation (United States); the Science and Technology Facilities Council (United Kingdom); the National Research Council (Canada); CONICYT (Chile); the Australian Research Council (Australia); Ministério da Ciência, Tecnologia e Inovação (Brazil); and Ministerio de Ciencia, Tecnología e Innovación Productiva (Argentina). A.Z. is supported by contract research *Internationale Spitzenforschung II-1* of the Baden-Württemberg Stiftung.

REFERENCES

Anders, E., & Grevesse, N. 1989, Geochim. Cosmochim. Acta, 53, 197
Begelman, M. C., Blandford, R. D., & Rees, M. J. 1980, Nature, 287, 307
Boylan-Kolchin, M., Ma, C.-P., & Quataert, E. 2004, ApJ, 613, L37
Bruzual, G., & Charlot, S. 2003, MNRAS, 344, 1000
Cappellari, M., & Emsellem, E. 2004, PASP, 116, 138
Carollo, C. M., Franx, M., Illingworth, G. D., & Forbes, D. 1997, ApJ, 481, 710
Coe, D., Umetsu, K., Zitrin, A., et al. 2012, ApJ, in press (arXiv:1201.1616)
Condon, J. J., Cotton, W. D., Greisen, E. W., et al. 1998, AJ, 115, 1693
Croft, S., de Vries, W., & Becker, R. H. 2007, ApJ, 667, L13
Diaferio, A., & Geller, M. J. 1997, ApJ, 481, 633
Diaferio, A., Geller, M. J., & Rines, K. J. 2005, ApJ, 628, L97
Dressler, A. 1989, in IAU Symp. 134, Active Galactic Nuclei, ed. D. E. Osterbrock & J. S. Miller (Dordrecht: Kluwer), 217
Ebisuzaki, T., Makino, J., & Okumura, S. K. 1991, Nature, 354, 212
Faber, S. M., Tremaine, S., Ajhar, E. A., et al. 1997, AJ, 114, 1771
Ferrarese, L., & Merritt, D. 2000, ApJ, 539, L9
Gebhardt, K., Bender, R., Bower, G., et al. 2000, ApJ, 539, L13
Gilmour, R., Best, P., & Almaini, O. 2009, MNRAS, 392, 1509
Graham, A. W. 2004, ApJ, 613, L33
Gualandris, A., & Merritt, D. 2008, ApJ, 678, 780
Gültekin, K., Richstone, D. O., Gebhardt, K., et al. 2009, ApJ, 698, 198
Hlavacek-Larrondo, J., Fabian, A. C., Edge, A. C., & Hogan, M. T. 2012, MNRAS, 424, 224
Hoffer, A. S., Donahue, M., Hicks, A., & Barthelemy, R. S. 2012, ApJS, 199, 23
Holley-Bockelmann, K., & Richstone, D. O. 2000, ApJ, 531, 232
Kormendy, J., & Bender, R. 2009, ApJ, 691, L142
Kormendy, J., & Richstone, D. 1995, ARA&A, 33, 581
Laine, S., van der Marel, R. P., Lauer, T. R., et al. 2003, AJ, 125, 478
Lauer, T. R. 1985, ApJS, 57, 473
Lauer, T. R. 1986, ApJ, 311, 34
Lauer, T. R., Ajhar, E. A., Byun, Y.-I., et al. 1995, AJ, 110, 2622
Lauer, T. R., Faber, S. M., Ajhar, E. A., Grillmair, C. J., & Scowen, P. A. 1998, AJ, 116, 2263
Lauer, T. R., Faber, S. M., Gebhardt, K., et al. 2005, AJ, 129, 2138
Lauer, T. R., Faber, S. M., Richstone, D., et al. 2007a, ApJ, 662, 808
Lauer, T. R., Gebhardt, K., Faber, S. M., et al. 2007b, ApJ, 664, 226
Lauer, T. R., Gebhardt, K., Richstone, D., et al. 2002, AJ, 124, 1975
Lucy, L. B. 1974, AJ, 79, 745
Magorrian, J., Tremaine, S., Richstone, D., et al. 1998, AJ, 115, 2285
Makino, J. 1997, ApJ, 478, 58
Maughan, B. J., Jones, C., Forman, W., & Van Speybroeck, L. 2008, ApJS, 174, 117
McConnell, N. J., Ma, C.-P., Gebhardt, K., et al. 2011, Nature, 480, 215
McNamara, B. R., Kazemzadeh, F., Rafferty, D. A., et al. 2009, ApJ, 698, 594
Merloni, A., Heinz, S., & di Matteo, T. 2003, MNRAS, 345, 1057
Merritt, D. 2006, ApJ, 648, 976
Merritt, D., Milosavljević, M., Favata, M., Hughes, S. A., & Holz, D. E. 2004, ApJ, 607, L9
Merritt, D., Schnittman, J. D., & Komossa, S. 2009, ApJ, 699, 1690
Milosavljević, M., & Merritt, D. 2001, ApJ, 563, 34
Milosavljević, M., Merritt, D., Rest, A., & van den Bosch, F. C. 2002, MNRAS, 331, L51
Postman, M., Coe, D., Benítez, N., et al. 2012, ApJS, 199, 25
Postman, M., & Lauer, T. R. 1995, ApJ, 440, 28
Quillen, A. C., Bower, G. A., & Stritzinger, M. 2000, ApJS, 128, 85
Ravindranath, S., Ho, L. C., & Filippenko, A. V. 2002, ApJ, 566, 801
Ravindranath, S., Ho, L. C., Peng, C. Y., Filippenko, A. V., & Sargent, W. L. W. 2001, AJ, 122, 653
Redmount, I. H., & Rees, M. J. 1989, Comments Astrophys., 14, 165
Rest, A., van den Bosch, F. C., Jaffe, W., et al. 2001, AJ, 121, 2431
Richardson, W. H. 1972, J. Opt. Soc. Am., 62, 55
Sánchez-Blázquez, P., Peletier, R. F., Jiménez-Vicente, J., et al. 2006, MNRAS, 371, 703
Vazdekis, A., Sánchez-Blázquez, P., Falcón-Barroso, J., et al. 2010, MNRAS, 404, 1639
White, R. L., Becker, R. H., Helfand, D. J., & Gregg, M. D. 1997, ApJ, 475, 479